Materials Letters 188 (2017) 176–179

Contents lists available at ScienceDirect

Materials Letters

journal homepage: www.elsevier.com/locate/matlet

Fabrication and electrochemical behavior study of nano-fibrous sodium titanate composite

Yeqian Ge[a,b,c,*], Jiadeng Zhu[b], Mahmut Dirican[b,d], Hao Jia[b], Meltem Yanilmaz[b], Yao Lu[b], Chen Chen[b], Yiping Qiu[c], Xiangwu Zhang[b,**]

[a] College of Textiles and Garments, Shaoxing University, Shaoxing 312000, China
[b] Department of Textile Engineering, Chemistry and Science, North Carolina State University, Raleigh, NC 27695-8301, USA
[c] Department of Textile Materials Science and Product Design, College of Textile, Donghua University, Shanghai 201620, China
[d] Department of Materials Science and Nanotechnology Engineering, Abdullah Gül University, Kayseri, Turkey

ARTICLE INFO

Keywords:
Sodium titanate
Nanocomposites
Electrospinning
Sodium-ion batteries
Electrochemical properties

ABSTRACT

Nanofiber structured $Na_2Ti_3O_7$ was synthesized via electrospinning process which was further used as an anode material for sodium-ion batteries for the first time. One-dimensional construction of $Na_2Ti_3O_7$ composite could contribute to better electrochemical activity. It was demonstrated that the capacity of $Na_2Ti_3O_7$ nanofibers was significantly improved to 257.8 mAh g^{-1} at 30 mA g^{-1}. Furthermore, the rate capability of $Na_2Ti_3O_7$ nanofibers was significantly enhanced, showing charge capacities were 161.8, 116.5, and 72.4 mAh g^{-1} at 100, 200, and 400 mA g^{-1}, respectively. Therefore, improved specific capacity and rate capability made $Na_2Ti_3O_7$ nanofibers composite as a promising anode material for sodium-ion batteries.

1. Introduction

The intensive depletion of fossil fuels brings about energy and environment concerns throughout the world. Aim to release the tension of this crisis, massive renewable energy are being explored, such as solar energy, nuclear energy. Meanwhile, to save these energy, relevant energy storage devices should also be developed. Rechargable batteries are widely used in portable devices, and now have been expanded to electronic vehicles, even large-scale energy storage systems, etc. [1,2]. Compared with lithium-ion batteries, sodium-ion batteries possess features of low cost and abundant sodium resource, having great potential to be applied particularly in the large-scale energy storage field [3,4]. Many efforts have been devoted to pursue a proper anode material for sodium-ion batteries, since graphite, the most common-use anode material in lithium-ion batteries, has little ability to store sodium ions in its layer structure due to the relatively larger radius of Na ions [5].

Titanium-based oxide insertion materials are considered with good chemical stability, good safety and sufficient resource in electrochemical utilization [6]. Among which, sodium titanate ($Na_2Ti_3O_7$) is drawing attention to the potential usage in sodium-ion batteries because it has the lowest insertion voltage (0.3 V vs. Na^+/Na). It is found that theoretically 1 M $Na_2Ti_3O_7$ can reversibly react with 2 M Na ions to achieve a capacity of 178 mAh g^{-1} [7]. However, the practical capacity of bulk $Na_2Ti_3O_7$ is restricted because of the sluggish kinetics. By designing into nanosize, the specific surface area of energy materials are enlarged. In addition, nanosize structure can reduce ion and charge transportation distance, leading to faster ion diffusion and charge transfer. Particularly, nanofiber structure can provide electron transfer network pathway, resulting in better electronic conductivity [4,8–10]. However, not much work has been done on $Na_2Ti_3O_7$ exploration in battery field. Table 1 presented the electrochemical properties of reported $Na_2Ti_3O_7$.

Herein, for the first time, we proposed a nanofiber structured $Na_2Ti_3O_7$ by using electrospinning method and thermal treatment, applying it as anode material for sodium-ion batteries. As a result, the charge-discharge capacity and rate capability were significantly improved.

2. Experimental sections

2.1. Materials synthesis

The processing of sodium titanate nanofibers was shown in Fig. 1a. An amount of 6.76 g $Ti(OC_4H_9)_4$ (Aldrich, 97%) was added dropwise to a polymer solution with 1 g poly(vinyl pyrrolidone) (PVP, Thermo

* Corresponding author at: College of Textiles and Garments, Shaoxing University, Shaoxing 312000, China.
** Corresponding author.
E-mail addresses: yge3@ncsu.edu (Y. Ge), yge3@ncsu.edu (X. Zhang).

http://dx.doi.org/10.1016/j.matlet.2016.11.025
Received 23 July 2016; Received in revised form 26 October 2016; Accepted 7 November 2016
Available online 10 November 2016
0167-577X/

Table 1
Electrochemical property comparison of $Na_2Ti_3O_7$ in this work with reported $Na_2Ti_3O_7$.

	Reversible capacity (mAh g^{-1} at mA g^{-1})	Rate capability (mAh g^{-1} at mA g^{-1})
$Na_2Ti_3O_7$/C particles [14]	178 at 35.6	55 at 14240
$Na_2Ti_3O_7$ particles [16]	177 at 17.8	71 at 890
$Na_2Ti_3O_7$ nanotubes [17]	205 at 400	100 at 3000
$Na_2Ti_3O_7$ nanoparticles [13]	188 at 17.8	64 at 356
$Na_2Ti_3O_7$ nanorods [18]	Around 200 at 17.8	Around 140 at 89
Microspheric $Na_2Ti_3O_7$ [19]	Around 177 at 354	Around 90 at 3540
$Na_2Ti_3O_7$ nanofibers (this work)	242.3 at 30	72.4 at 400

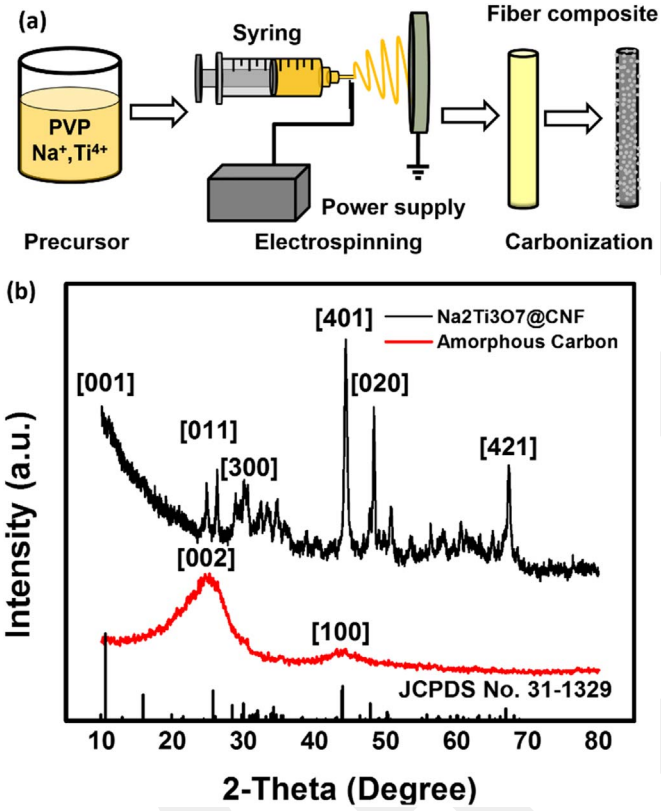

Fig. 1. (a) Schematic illustration of the fabrication process of $Na_2Ti_3O_7$ nanofibers. (b) XRD patterns of $Na_2Ti_3O_7$ nanofibers and amorphous carbon.

Fisher Scientific, Mw=1,300,000 g mol^{-1}) in solvent of 14 g C_2H_5OH, (Aldrich, ≥99%) and 1.2 g CH_3COOH (Aldrich, ≥99%). Then 1.196 g CH_3COONa (Aldrich, ≥99%) was also added into the solution with vigorous stirring for two days at around 1000 r/min. Then the precursor solution was spun on an electrospinning setup with a voltage of 20 kV, flow rate of 0.75 ml h^{-1} and a tip-to-collector distance of 15 cm. The nanofiber mat was stabilized in air at 280 °C for 5.5 h then further treated in nitrogen at 750 °C for 4 h [3,4]. During processing, PVP was pyrolyzed into amorphous carbon and $Na_2Ti_3O_7$ could be synthesized [3,17], therefore, $Na_2Ti_3O_7$ nanofiber contained carbon ingredient. As comparison, pure $Na_2Ti_3O_7$ particles were also produced by sol-gel method from the same solution as $Na_2Ti_3O_7$ nanofibers. The solution was first dried in the oven at 50 °C overnight and then sintered at 750 °C for 4 h in air.

2.2. Structural and morphologic characterization

The morphology of $Na_2Ti_3O_7$ samples were observed by field-emission scanning electron microscopy (FE-SEM, FEI VERIOS 460 L) and transmission electron microscopy (TEM and HRTEM, Hitachi HF 2000, accelerating voltage 200 kV). The lattice structure of $Na_2Ti_3O_7$ nanofiber was confirmed with standard file by using wide-angle X-ray diffractometer (WAXD, Rigaku Smartlab). The carbon content was conducted by elemental analysis (EA, Perkin Elmer 2400 Series II CHNS/O Elemental Analyzer).

2.3. Electrochemical characterization

Sodium titanate samples were assembled into CR2032 coin cells. The electrode was making from slurry onto copper foil, which composed of active material, carbon black and sodium alginate binder in deionized water with the weight ratio 8:1:1. The mass loading of the active material was around 1 mg cm^{-2}. The electrode was punched into half-inch circles and heated in the oven at 100 °C overnight before using. The counter electrode was sodium slice. Electrolyte was made of 1 M $NaClO_4$ (98%) dissolved in ethylene carbonate (98%) and dimethyl carbonate (≥99%) (1:1 by volume). Glass fiber mat (Whatman) was used as the separator. All the assembling process was completed in an argon-filled glove box. Charge-discharge performance and rate capability at a voltage range of 0–2.5 V (vs. Na/Na^+) were carried galvanostatically on a LAND (CT2001A) battery testing system. With the scan rate of 0.1 mV s^{-1}, CV feature of $Na_2Ti_3O_7$ nanofibers were described by Reference 600 Potentiostat/Galvanostat/ZRA (GAMRY).

3. Results and discussion

The XRD spectrum of $Na_2Ti_3O_7$ nanofibers from 10 to 80° was exhibited in Fig. 1b. Notably, main diffraction peaks at 10.56°, 25.76°, 29.64°, 39.78°, 47.48°, and 66.96° were appeared, which could be indexed to the [001], [011], [300], [400], [020], and [421] crystal planes of $Na_2Ti_3O_7$ presented in JCPDS No. 31–1329 [11]. The curve had very strong slope at the beginning, which was resulted from the background signal. However, the XRD peak intensity and resolution of $Na_2Ti_3O_7$ nanofibers were low, which was attributed to the introduction of amorphous carbon [12]. The carbon content of $Na_2Ti_3O_7$ nanofibers were detected with 5.82%. The XRD curve of pure carbon pyrolyzed from PVP was also provided as comparison, presenting broad peaks at around 26° and 43°, corresponding to the [002] and [100] phase of the graphitized structure [3].

The morphology of $Na_2Ti_3O_7$ particles and nanofibers was observed by SEM. Fig. 2a and b demonstrated $Na_2Ti_3O_7$ particles were agglomerated into bigger bulk. The average particle size of primary and secondary particles were around 0.93 μm and 20 μm, respectively. As to $Na_2Ti_3O_7$ nanofibers, distinct fine nano-fibrous structure with around 140 nm in diameter were exhibited in Fig. 2c and d. In order to confirm the structure of $Na_2Ti_3O_7$ nanofiber, TEM and HRTEM were also illustrated in Fig. 2e and f. The nanofiber was composed with amorphous and crystal phases, indicated carbon and $Na_2Ti_3O_7$ crystal. In addition, the lattice spacing indexed in HRTEM images was 5.59 Å for [101] lattice planes of $Na_2Ti_3O_7$, agreed with the XRD result.

The first three charge-discharge curves of $Na_2Ti_3O_7$ particles and nanofibers at 30 mA g^{-1} were recorded between 0 and 2.5 V (vs. Na/Na^+), shown in Fig. 3a and b. Notably, electrochemical activity of $Na_2Ti_3O_7$ particles was limited. At the first cycle, the discharge capacity and charge capacity were only 96.3 mAh g^{-1} and 52.3 mAh g^{-1}, respectively, which indicated that 45.7% of sodium ions became irreversible during this cycling. In contrast, $Na_2Ti_3O_7$ nanofibers demonstrated a charge capacity of 257.8 mAh g^{-1} at the first cycle, which was 5 times higher than that of $Na_2Ti_3O_7$ particles. In order to further understand the electrochemical reaction of $Na_2Ti_3O_7$ nanofibers, CV measurements were conducted on Gamry tester. According to

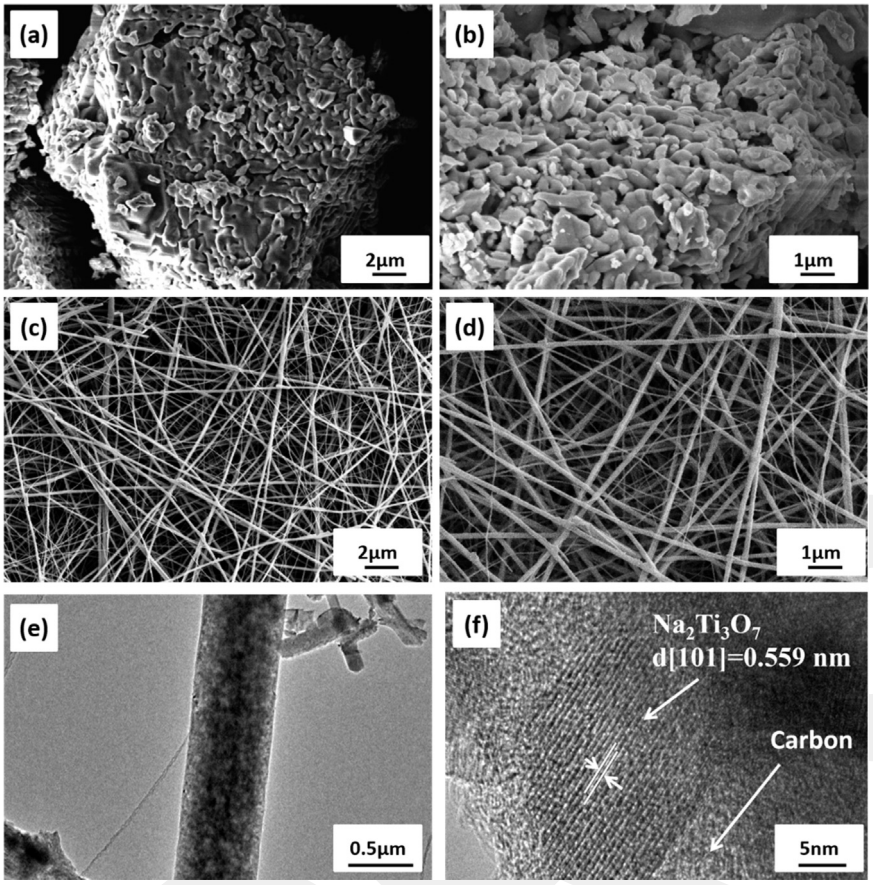

Fig. 2. SEM of (a, b) $Na_2Ti_3O_7$ particle, (c, d) $Na_2Ti_3O_7$ nanofibers, (e, f) TEM and HRTEM of $Na_2Ti_3O_7$ nanofibers.

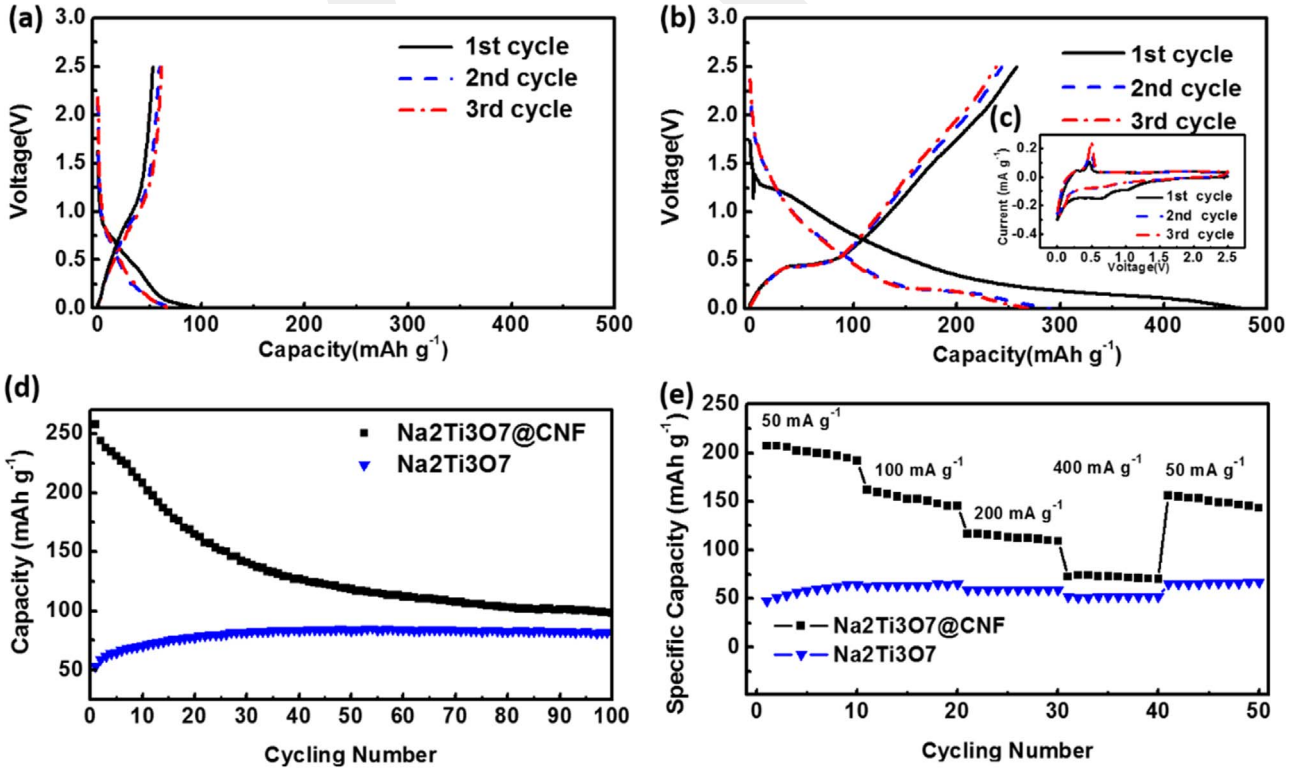

Fig. 3. Charge-discharge curves of (a) $Na_2Ti_3O_7$ particles, (b) $Na_2Ti_3O_7$ nanofibers, inserted (c) CV curves of $Na_2Ti_3O_7$ nanofibers. (d) Cycling performance and (e) Rate capability of $Na_2Ti_3O_7$.

inserted Fig. 3c, there were two cathodic peaks at 0.659 V and 1.02 V in the first cycle, but they were disappeared at the following cycles which was due to the electrolyte irreversible decomposition. Another cathodic peaks at around 0 V in each cycles referred to the Na ions insertion into active material [13]. Besides, all three cycles exhibited an anodic peak at around 0.49 V, which was related to the reversible oxidation of Ti^{3+}/Ti^{4+}. It has been suggested that the forms of $Na_2Ti_3O_7$ and $Na_4Ti_3O_7$ are reversibly converted during Na^+ intercalation and extraction, involving Ti^{3+} vs Ti^{4+} transition [14,15].

Fig. 3d showed the galvanostatic cycling performance of $Na_2Ti_3O_7$ particles and nanofibers for 100 cycles at 30 mA g^{-1}. The initial charge capacity of $Na_2Ti_3O_7$ nanofiber composite was 257.8 mAh g^{-1}, and it remained 98.6 mAh g^{-1} after 100 cycles. While it was only 53.2 mAh g^{-1} and 82 mAh $g^{-1}$for $Na_2Ti_3O_7$ particles respectively. $Na_2Ti_3O_7$ nanofibers had higher capacity but the capacity retention was not such good. The possible reason was nanosized $Na_2Ti_3O_7$ having more side-reactions with larger Na consumption at low current density, and $Na_2Ti_3O_7$ was found with poor stability because of structure deformation. Therefore, the nanosize framework could improve the capacity but at the same time might lead to structure distortion more easily [13,14]. Notably, the capacity of $Na_2Ti_3O_7$ particles was slightly increased. The reason might be the aggregated cluster of $Na_2Ti_3O_7$ particles would prevent electrolyte permeation and delay the ion conductivity. With time passing by, the electrolyte would permeate into the primary structure.

Remarkably, $Na_2Ti_3O_7$ nanofibers presented outstanding rate performance, compared with $Na_2Ti_3O_7$ particles, shown in Fig. 3e. The rate capabilities were tested at current densities of 50, 100, 200, and 400 mA g^{-1}, and then back to 50 mA g^{-1}. The charge capacities of $Na_2Ti_3O_7$ nanofibers were 206.9, 161.8, 116.5, and 72.4 mAh g^{-1}, respectively. When the current density was back to 50 mA g^{-1}, the charge capacities returned to 156.3 mAh g^{-1}. At the same condition, the charge capacities of $Na_2Ti_3O_7$ particles were only 48.1, 62.6, 59.2, and 52.0 mAh g^{-1}, respectively.

4. Conclusions

In summary, $Na_2Ti_3O_7$ nanofibers were successfully produced by using electrospinning process and thermal treatment. $Na_2Ti_3O_7$ nanofibers demonstrated higher charge capacity than $Na_2Ti_3O_7$ particles, which achieved as high as 257.8 mAh g^{-1}. Preferably, $Na_2Ti_3O_7$ nanofibers exhibited good rate capability. The charge capacities of $Na_2Ti_3O_7$ nanofibers were 206.9, 161.8, 116.5, and 72.4 mAh g^{-1} at 50, 100, 200, and 400 mA g^{-1}, respectively. Therefore, $Na_2Ti_3O_7$ nanofibers could be a candidate in practical sodium-ion batteries anode material.

Acknowledgments

The work was supported by the Scientific Research Staring Foundation of Shaoxing University (No. 20165006). The authors appreciated Yang Liu (AIF facility manager, NCSU) and Lisa Lentz (NCSU) providing great help for this work.

References

[1] J. Zhu, Y. Lu, C. Chen, Y. Ge, S. Jasper, J.D. Leary, D. Li, M. Jiang, X. Zhang, Porous one-dimensional carbon/iron oxide composite for rechargeable lithium-ion batteries with high and stable capacity, J. Alloy. Compd. 672 (2016) 79–85.
[2] J. Zhu, C. Chen, Y. Lu, Y. Ge, H. Jiang, K. Fu, X. Zhang, Nitrogen-doped carbon nanofibers derived from polyacrylonitrile for use as anode material in sodium-ion batteries, Carbon 94 (2015) 189–195.
[3] Y. Ge, H. Jiang, J. Zhu, Y. Lu, C. Chen, Y. Hu, Y. Qiu, X. Zhang, High cyclability of carbon-coated TiO_2 nanoparticles as anode for sodium-ion batteries, Electrochim. Acta 157 (2015) 142.
[4] Y. Ge, J. Zhu, Y. Lu, C. Chen, Y. Qiu, X. Zhang, The study on structure and electrochemical sodiation of one-dimensional nanocrystalline TiO_2@C nanofiber composites, Electrochim. Acta 176 (2015) 989–996.
[5] P. Ge, M. Fouletier, Electrochemical intercalation of sodium in graphite, Solid State Ion. 28 30 (1988) 1172.
[6] Y. Jiang, M. Hu, D. Zhang, T. Yuan, W. Sun, B. Xu, M. Yan, Transition metal oxides for high performance sodium ion battery anodes, Nano Energy 5 (2014) 60.
[7] P. Senguttuvan, G. Rousse, V. Seznec, J.-M. Tarascon, M.R. Palacín, $Na_2Ti_3O_7$: lowest Voltage Ever Reported Oxide Insertion Electrode for Sodium Ion Batteries, Chem. Mater. 23 (2011) 4109–4111.
[8] L. Ji, Z. Lin, M. Alcoutlabi, X. Zhang, Recent developments in nanostructured anode materials for rechargeable lithium-ion batteries, Energy Environ. Sci. 4 (2011) 2682–2699.
[9] J. Yin, L. Qi, H. Wang, Sodium titanate nanotubes as negative electrode materials for sodium-ion capacitors, ACS Appl. Mater. Interfaces 4 (2012) (2762-8).
[10] B. Fu, X. Zhou, Y. Wang, Co_3O_4 carbon nanofiber mats as negative electrodes for sodium-ion batteries, Mater. Lett. 170 (2016) 21–24.
[11] Z. Yan, L. Liu, H. Shu, X. Yang, H. Wang, J. Tan, Q. Zhou, Z. Huang, X. Wang, A tightly integrated sodium titanate-carbon composite as an anode material for rechargeable sodium ion batteries, J. Power Sour. 274 (2015) 8.
[12] Y. Ge, H. Jiang, K. Fu, C. Zhang, J. Zhu, C. Chen, Y. Lu, Y. Qiu, X. Zhang, Copper-doped $Li_4Ti_5O_{12}$/carbon nanofiber composites as anode for high-performance sodium-ion batteries, J. Power Sour. 272 (2014) 860.
[13] H.L. Pan, X. Lu, X.Q. Yu, Y.S. Hu, H. Li, X.Q. Yang, L.Q. Chen, Sodium storage and transport properties in layered $Na_2Ti_3O_7$ for room-temperature sodium-ion batteries, Adv. Energy Mater. 3 (2013) 1186.
[14] A. Rudola, N. Sharma, P. Balaya, Introducing a 0.2V sodium-ion battery anode: the $Na_2Ti_3O_7$ to $Na_{3-x}Ti_3O_7$ pathway, Electrochem. Commun. 61 (2015) 10–13.
[15] G. Rousse, M.E. Arroyo-de Dompablo, P. Senguttuvan, A. Ponrouch, J.-M. Tarascon, M.R. Palacín, Rationalization of intercalation potential and redox mechanism for $A_2Ti_3O_7$(A=Li, Na), Chem. Mater. 25 (2013) 4946–4956.
[16] A. Rudola, K. Saravanan, C.W. Mason, P. Balaya, $Na_2Ti_3O_7$: an intercalation based anode for sodium-ion battery applications, J. Mater. Chem. A 1 (2013) 2653.
[17] Y. Zhang, L. Guo, S. Yang, Three-dimensional spider-web architecture assembled from $Na_2Ti_3O_7$ nanotubes as a high performance anode for a sodium-ion battery, Chem. Commun. 50 (2014) 14029–14032.
[18] W. Wang, C. Yu, Y. Liu, J. Hou, H. Zhu, S. Jiao, Single crystalline $Na_2Ti_3O_7$ rods as an anode material for sodium-ion batteries, RSC Adv. 3 (2013) 1041.
[19] W. Wang, C. Yu, Z. Lin, J. Hou, H. Zhu, S. Jiao, Microspheric $Na_2Ti_3O_7$ consisting of tiny nanotubes: an anode material for sodium-ion batteries with ultrafast charge-discharge rates, Nanoscale 5 (2013) 594.